Theor Chem Acc (2003) 109:268–273
DOI 10.1007/s00214-002-0420-4

Theoretical
Chemistry Accounts

Regular article

An ab initio study of the structure of two-, three- and five-dimer silicon clusters: An approach to the Si(100) surface

Yousung Jung[1,3], Yoshinubu Akinaga[1], Kenneth D. Jordan[2], Mark S. Gordon[1]

[1] Department of Chemistry, Iowa State University, Ames, IA 50011
[2] Department of Chemistry, University of Pittsburgh, Pittsburgh, PA 15260
[3] Department of Chemistry, University of California, Berkeley, CA

Received: 9 November 2001 / Accepted: 6 September 2002 / Published online: 4 April 2003

Abstract. Two-, three- and five-dimer cluster models were used to elucidate the structures of small models of the Si(100) surface. Because surface dimers have been shown to have significant singlet diradical character, multi-reference wave functions were used in order to obtain a reliable description of such species. CASSCF (complete active space SCF) geometry optimizations find symmetric structures to be the global minima, with no local minima at buckled structures. This result for the three- and five-dimer clusters implies that dimer– dimer repulsions are not sufficient to cause buckling of these species. These results are in contrast with most previous calculations that predict buckling of surface dimers. The effect of the dynamic part of the electron correlation on surface structure was assessed by performing single point multi-reference perturbation theory (MRMP) calculations along the three buckling normal modes of the three-dimer cluster. Although dynamic correlation effects are found to "soften" motion along the buckling coordinates, the surface remains unbuckled when such correlation effects are included. The MRMP results are in qualitative agreement with the CASSCF predictions. The implications of these results with regard to the structure of the Si(100) surface are discussed.

Keywords: MCSCF – Si (100) – Clusters

Introduction

The Si(100) surface has been the subject of many experimental and theoretical studies [1, 2, 3, 4, 5, 6, 7] due to its importance in the semiconductor industry. These studies have revealed many aspects of the silicon surface including the fact that the Si(100) surface reconstructs, after being cleaved, to form dimers. The experimental bond length of the dimer suggests that the Si-Si bonding in this species is intermediate between those that are typical of a single and double bond. Several computational studies have demonstrated that these dimers have significant diradical character with ~1/3 of an electron occupying the lowest unoccupied molecular orbital (LUMO) in each dimer. This suggests that single-determinant wave functions (e.g. Hartree–Fock and most of the popular implementations of density functional theory (DFT)) are unlikely to provide a reliable description of the structure and bonding of such species, since they cannot account for the significant electron density in the dimer antibonding orbitals. It is therefore essential, when using clusters to describe the Si(100) surface, to use a proper wave function as a starting point.

There are several intriguing questions regarding the Si(100) surface:

i. Are the Si(100) surface dimers buckled or symmetric?
ii. Does dynamic correlation play an important qualitative role in determining the structure of the surface?
iii. Do dimer-dimer interactions affect the structure of the surface?

The physical nature of the Si(100) surface has important implications with regard the underlying origins of reaction mechanisms on the surface, since a physically buckled surface could result in different chemical environments for the two Si atoms in a dimer.

Even those theoretical studies that predict surface buckling give a relatively small stabilization (~0.1 eV per dimer) due to the buckling. Thus, it is clear from the outset that a carefully balanced treatment of electron correlation effects is necessary to definitively resolve the question of whether the surface is buckled.

Electron correlation energy is typically defined as the difference between the "exact" non-relativistic energy and the energy at the Hartree–Fock limit, achieved by using an infinite basis set. Non-dynamic (or internal) electron correlation refers to the electron correlation

---

Correspondence to: M. S. Gordon
e-mail: mark@si.fi.ameslab.gov

that can be recovered by adding flexibility to the wave function, when there are near degeneracies or when the gap between HOMO and LUMO is small enough to permit configurational mixing. The MCSCF (multi-configurational SCF) [8] method is typically used for recovering the non-dynamic electron correlation. The remaining electron correlation is called dynamic correlation, even though there is no rigorous way to separate these two effects. Many body perturbation theory and configuration interaction (CI) are the most common methods to account for dynamic correlation. It can be argued that density functional theory also accounts for some dynamic correlation, since most modern functionals include a correlation component. It is difficult, however, to assess this effect quantitatively, particularly for functionals that contain parameters that are fitted to experimental results. Multi-reference perturbation theory (MRMP) is a commonly used method for including both dynamic and non-dynamic correlation effects.

Redondo and Goddard [9] were the first to show that, because surface dimers exhibit partial diradical character (significant population of the LUMO), a single reference wave function is not sufficient for an adequate description of the Si(100) dimerized surface, and a multi-reference (e.g. MCSCF) wave function is necessary. A simple way to determine whether or not a system needs a multi-reference wave function is to examine the restricted Hartree-Fock (RHF) orbital energies. When the LUMO orbital energy is negative, the system is frequently multi-configurational and needs a non-dynamic electron correlation correction. Indeed, this is the case for the clusters that are typically used to represent the reconstructed Si(100) surface. Recent studies [9, 10, 11, 12] using cluster models and MCSCF-based methods have predicted that the Si(100) surface dimers are symmetric (or 'unbuckled'), while single reference methods such as Hartree–Fock or density functional theory (DFT) [13, 14, 15, 16, 17] have generally predicted the only potential energy minimum to be a buckled structure.

Recently, Hess and Doren [13] argued that dynamic correlation plays a significant role in determining the structure of small clusters used to represent the surface and even alters the relative stabilities of buckled and symmetric structures to favor a buckled structure. They optimized a Si_9H_{12} single dimer cluster with both DFT and complete active space (CAS) SCF including four electrons in four orbitals, CASSCF(4,4), methods. They found that DFT optimization gives a buckled structure, while CASSCF(4,4) optimization predicts a symmetric (C_{2v}) structure as a minimum. Single point MRMP calculations at both the DFT-optimized buckled structure and the CASSCF-optimized symmetric structure predicted the buckled structure to be slightly lower (0.9 kcal/mol) in energy than the symmetric one. Based on these single point MRMP calculations, they concluded that the structure of Si_9H_{12} is buckled and dynamic correlation plays an important role in determining the structure. Of course, a comparison of energies of two different geometries that were obtained from different levels of theory may not be reliable, especially where the energy difference is quite small.

Ideally, one should optimize the structure of the clusters at the MRMP level of theory in order to include the effects of both dynamic and non-dynamic correlation on the predicted structure. Unfortunately, MRMP analytic gradients are not yet available, and numerical geometry optimizations of clusters of the size of interest here would be computationally too demanding. One alternative is to distort the cluster along the CASSCF buckling mode(s) and to perform MRMP calculations along the resulting potential energy curve. Following the procedure for the single dimer Si_9H_{12} cluster. Gordon, Shoemaker, and Burggraf found that the MRMP energy increases monotonically along the buckling mode, qualitatively in agreement with CASSCF results. They also performed a single reference MP2 geometry optimization starting from both symmetric and buckled structures, and found only a symmetric dimer structure. They therefore concluded that the Si(100) surface is symmetric within a Si_9H_{12} cluster model at 0 K, and that dynamic correlation does not have a qualitatively important effect on the predicted geometry. Although this cluster model is clearly too small to provide a realistic description of the Si(100) surface, these results clearly demonstrate that density functional methods are biased toward buckled structures.

It has also been suggested [14, 15, 16] that interactions between adjacent dimers in the same row may have a stabilizing effect on the buckled structure. These DFT calculations indicate that a buckled structure gains extra stability due to dimer–dimer interactions (one Si atom of a dimer is pointing up and the other pointing down in one dimer, with adjacent dimers buckled in the opposite direction). This stabilization has been estimated to be 1.5~3 kcal/mol per dimer in a two-dimer model and 3.5~4.5 kcal/mol in a three-dimer cluster model. On the contrary, recent multi-reference CI calculations using a two-dimer cluster model [10] still predict a symmetric structure as a minimum, implying that dimer-dimer interactions may be over-estimated in DFT calculations.

One may also question whether a cluster of any computationally tractable size can adequately model the Si(100) surface and if so, what an appropriate cluster size might be? An alternative approach, using slab models and periodic boundary conditions, is often considered to be more representative of the surface site interactions than cluster models, as long as the supercells of the slab models maintain a reasonable periodicity. A recent DFT study on H_2 desorption from the Si(100) surface using both slab and cluster models [18] has found that the reaction and activation energy for H_2 desorption for the monohydride of the Si(100) surface calculated using a three-dimer cluster are close to the results predicted by the slab model.

To the best of our knowledge, clusters containing more than two dimers have not yet been studied using the combined MCSCF and MRMP methods. The present work examines the structure of the surface systematically by increasing the size of the cluster (the number of dimers) up to five dimers, in order to provide some insight regarding the effect of dimer–dimer interactions, if any, on the structure of the surface dimers. As an extension of the Si_9H_{12} cluster study [11, 12], two-dimer ($Si_{15}H_{16}$), three–dimer ($Si_{20}H_{21}$) and five-dimer ($Si_{33}H_{28}$) clusters are analyzed with CASSCF(4,4), CASSCF(6,6) and CASSCF(10,10) wave functions, respectively. (The $Si_{33}H_{28}$ clsuter model is depicted in Fig. 1). In addition, MRMP calculations are carried out on the two- and three-dimer cluster models.

Computational details

Two-dimer ($Si_{15}H_{16}$), three-dimer ($Si_{20}H_{21}$) and five-dimer ($Si_{33}H_{28}$) clusters were used to model the structure of the Si(100) surface. The 6–31G(d) [19] basis set was used for the $Si_{15}H_{16}$ cluster, and the HW(d) effective core potential (ECP) and basis set was used for $Si_{20}H_{21}$ and $Si_{33}H_{28}$ due to the size of the clusters. It has been shown in many papers [11, 20, 21] that HW(d) [22] calculations give a good description of the silicon surface, since it saves considerable computational cost by treating the core electrons of heavy atoms with fitted potentials and still gives reasonable results. The HW(d) basis comprises a –21G(d) basis for the valence shell electrons of Si atoms and the 21G basis for H atoms.

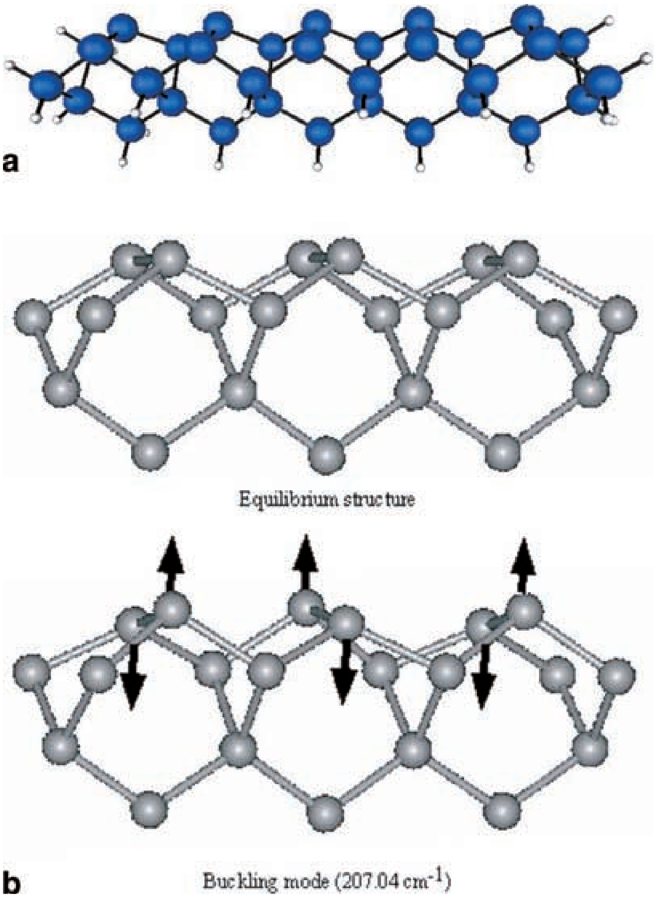

Fig. 1. **a** Equilibrium structure for 5-dimer cluster. **b** Equilibrium structure and buckling mode for 3-dimer cluster

Four active electrons and four active orbitals were used as an active space in the MCSCF [8] calculations for the two-dimer cluster, denoted by CASSCF(4,4), CASSCF(6,6) for the three-dimer cluster and CASSCF(10,10) for the five-dimer cluster. All of these active orbitals correspond to bonding and anti-bonding Si-Si surface dangling bond orbitals. The optimized two-dimer and three-dimer structures were characterized by computing and diagonalizing the Hessian matrices (matrix of energy second derivatives with respect to the nuclear coordinates). A minimum has a positive definite hessian and a transition state (or first order saddle point) has one negative eigenvalue. As discussed below, single point calculations were performed with second order multi-reference perturbation theory (MRMP2) [23].

The GAMESS electronic structure program [24] was used for all calculations reported here, making use of the parallel MCSCF codes [25, 26].

Results and discussion

All three clusters (two-, three- and five-dimers) are predicted to have only symmetric C_{2v} minima on their respective CASSCF potential energy surfaces. Starting from buckled structures predicted by density functional theory, CASSCF optimizations converged to symmetric dimers. These one- [12], two-, three- and five-dimer results suggest that dimer-dimer interactions are not large enough to lead to buckling in these cluster models of the Si(100) surface. This is especially noteworthy for the two largest clusters, since they have increasing numbers of dimers. The five-dimer cluster has interacting dimers that are not at the edges of the cluster.

The dimer bond lengths as a function of the size of the cluster are compared in Table 1. All cluster models using MCSCF wave functions predict the dimer bond length to be between 2.24 and 2.28 Å, very close to the experimental value (~2.26 Å [27]). In fact, since the Si_9H_{12} results suggest that ECPs underestimate the dimer distance by 0.04 Å, it is likely that the CASSCF/6–31G(d) level of theory would consistently predict a distance of 2.28 Å. In contrast, the RHF method [11] predicts a much smaller value of 2.18 Å. Because RHF (and other single determinant methods) cannot occupy the antibonding LUMO, the Si–Si bonding in the dimer is overestimated by over-emphasizing the Si–Si π bonding. On the other hand, a singlet UHF calculation yields a dimer Si–Si bond length of 2.32 Å, closer to the experimental value than RHF. The fact that the singlet UHF is distinct from the RHF wave function for this species, and the large spin contamination both suggest that a single configuration description is inadequate. Thus, we conclude that the bond length of the Si(100) surface dimer is independent of the size of the cluster

Table 1. Dimer bond lengths of the reconstructed Si(100) surface

Cluster model	Method	Length (Å)	Reference
One-dimer (Si_9H_{12})	RHF/HW(d)	2.18	Shoemaker et al.[a]
One-dimer (Si_9H_{12})	UHF/HW(d)[c]	2.32	This work
One-dimer (Si_9H_{12})	CASSCF(2,2)/6-31G(d)	2.28	Shoemaker et al.[a]
One-dimer (Si_9H_{12})	CASSCF(2,2)/HW(d)	2.24	Shoemaker et al.[a]
Two-dimer ($Si_{15}H_{16}$)	CASSCF(4,4)/6-31G(d)	2.28, 2.28	This work
Three-dimer ($Si_{20}H_{21}$)	CASSCF(6,6)/HW(d)	2.24, 2.25,2.24	This work
Five-dimer ($Si_{33}H_{28}$)	CASSCF(10,10)/HW(d)	2.24, 2.24,2.24	This work
Experiment	TOF SARS	2.26 ± 0.1	Wang et al.[b]

[a] Reference [11]
[b] Reference [44]
[c] Severe spin contamination is observed, $<S^2>_{\mathrm{UHF}} = 0.94$ ($<S^2>_{\mathrm{TRUE}} = 0.00$ for a singlet state)

model as long as an adequate multi-reference wave function is used.

Further evidence for the need for a multi-reference wave function is provided by the natural orbital occupation numbers (NOON) for the orbitals in the CASSCF active space. The natural orbitals are the eigenvectors of the first-order density matrix for any variational wave function (e.g. HF, CASSCF), and the corresponding eigenvalues are the NOON. In a single-reference wave function (e.g. HF, DFT) the NOON are 2.0 for the occupied (bonding) orbitals and 0.0 for the virtual (antibonding) orbitals. So, deviations from these values are measures of the adequacy or inadequacy of the single-reference wave function. For all of the dimers studied here, the NOON are ~1.65 electrons for the occupied orbitals and ~0.35 electrons for the virtual orbitals. This means that ~1/3 electron in *each dimer* occupies an orbital that is inaccessible in a single-reference wave function. In other words, a net 1.05 electrons in the three-dimer cluster and 1.67 electrons in the five-dimer cluster are not properly described by a single-reference wave function.

The effect of dynamic electron correlation on the structure of the surface was investigated by calculating single-point MRMP energies for displacements along the buckling vibrational normal modes. The symmetric structures found in the CASSCF geometry optimization were used for the vibrational frequency calculations. The number of buckling modes is equal to the number of surface dimers included in the calculation. Table 2 summarizes the CASSCF and MRMP2 results along each buckling mode. The main point that can be drawn from this table is that both CASSCF and MRMP2 energies monotonically increase as the surface dimers buckle along the buckling normal modes. In other words, MRMP2 does not change the qualitative CASSCF trend that the surface dimers are symmetric and increase in energy as the dimers buckle. The relative MRMP2 energies are somewhat lower than the relative CASSCF energies. However, these small quantitative changes do not alter the fundamental conclusion that dynamic correlation does not play a qualitative role in determining the structure of the surface dimers.

A more detailed analysis of the dimer–dimer interactions was obtained by examining the localized CASSCF active orbitals (LMOs) for the three-dimer cluster, using the Ruedenberg energy localization procedure [27, 28]. As noted by Ruedenberg and co-workers

Table 2. Relative CASSCF and MRMP2 energies (kcal/mol) along the CASSCF buckling normal modes

	Buckling modes	Min[a]	5%[b]	10%[b]	15%[b]	25%[b]	50%[b]	100%[b]
One-dimer (1 buckling mode)[c]								
TCSCF/6-31G(d)	191.34 cm^{-1}	0.00	0.04	0.15	0.33	0.93	3.68	14.06
MRMP2	191.34 cm^{-1}	0.00	0.02	0.10	0.21	0.60	2.40	10.08
Two-dimer (2 Buckling modes)								
CASSCF(4,4)/6-31G(d)	190.83 cm^{-1}	0.00	0.04	0.15	0.33	0.90	3.53	13.63
	192.65 cm^{-1}	0.00	0.00	0.11	0.31	0.93	3.81	14.92
MRMP2	190.83 cm^{-1}	0.00	0.02	0.07	0.17	0.46	1.85	7.48
	192.65 cm^{-1}	0.00	0.00	0.06	0.17	0.52	2.17	8.93
Three-dimer (3 Buckling Modes)								
CASSCF(6,6)/HW(d)	207.04 cm^{-1}	0.00	0.04	0.15	0.41	0.91	3.63	14.28
	207.26 cm^{-1}	0.00	0.04	0.17	0.38	1.05	4.18	16.38
	210.31 cm^{-1}	0.00	0.05	0.18	0.33	1.15	4.58	18.01
MRMP2	207.04 cm^{-1}	0.00	0.02	0.08	0.28	0.48	1.91	7.78
	207.26 cm^{-1}	0.00	0.03	0.11	0.24	0.67	2.68	10.96
	210.31 cm^{-1}	0.00	0.03	0.12	0.17	0.78	3.10	12.47

[a] Symmetric equilibrium structure
[b] Degree of distortion from the equilibrium surface geometry along the buckling vibrational modes. For example, 100% implies the geometry that corresponds to the maximum displacement along the buckling mode from the equilibrium structure
[c] Previous study by Gordon et al. [12]

[28, 29], localization of CASSCF orbitals leads to atomic-like orbitals. It is then possible to examine both the density matrix elements connecting these hybrid LMOs and the Coulomb and exchange repulsions between them. The former interactions provide information regarding the bonding or antibonding between hybrids, while the latter can be used to quantify any inter-dimer repulsions.

Figure 1 illustrates the lowest frequency (207.04 cm^{-1}) buckling mode for the three-dimer cluster. Density matrices for the CASSCF LMOs were calculated along this mode. All off-diagonal density matrix elements (i.e. bond orders) between LMOs on different Si–Si dimers are calculated to be very small (< 0.01) along the entire buckling mode. This means that at the CASSCF level of theory, the buckling motion does not affect the bonding or antibonding dimer–dimer interactions.

The coulomb and exchange repulsion integrals were also calculated between the localized orbitals on different dimers along the same buckling mode (Fig. 1). As one would expect, the repulsions between two adjacent dimers decrease as the dimers buckle. For the three- dimer cluster, the total decrease in the total repulsion energy is 8.78 kcal/mol. So, the dimer-dimer repulsions do indeed favor buckling. Since the levels of theory employed here predict a symmetric (unbuckled) structure, factors other than inter-dimer repulsions must be dominant.

It is interesting that many experiments have been interpreted as providing evidence for a buckled Si(100) surface [6, 7, 30, 31]. However, recently,Yokoyama et al. [32] conducted low temperature (63 K and 5 K) STM experiments and found a buckled surface structure with the *c*(4×2) reconstruction in the 63 K measurements, but that most dimers adopted symmetrical arrangements with *c*(2×1)-like periodicity in the 5 K measurements. It is possible that the buckling found in prior low-temperature measurements has been induced by defects. Defect-induced buckling has been invoked by Badt et al. in the interpretation of their STM measurements [33].

When we were in the final stages of preparing this manuscript, we became aware of a very interesting recent paper by Filippi et al. [34]. These authors performed diffusion Monte Carlo (DMC) calculations on the Si_9H_{12}, $Si_{15}H_{16}$, and $Si_{21}H_{20}$ cluster models at both planar and buckled geometries generated by Scheffler et al. using plane-wave density functional calculations. The DMC method, like the MRMP2 method employed in our study, includes both dynamical and non-dynamical electron correlation effects. A second similarity is that the DMC calculations were performed at plane wave DFT geometries (a method that favors buckling), just as the MRMP calculations were performed at CASSCF geometries (a method that favors symmetric structures). The DMC calculations are ambiguous concerning the buckling of the Si_9H_{12} cluster (since the energy difference is smaller than the uncertainties in the calculated energies), but they predict the DFT buckled structures of the two larger clusters to be more stable than the DFT planar structures. The preference for buckling is greater for the $Si_{21}H_{20}$ cluster.

Thus, two methods that include both dynamic and non-dynamic correlation effects lead to different conclusions concerning the buckling of these cluster models. However, an important point is that the DMC calculations give a smaller energy lowering upon buckling than do the DFT calculations. This supports our conclusion that DFT methods are biased toward buckled structures. Concerning the differences between the DMC and MRMP2 results, note that:

1. The two studies used different geometrical structures in addressing the buckling issue. In particular, the DMC structures were obtained by fixing the positions of the lower layers of the clusters. It has been pointed out previously [11] that such constraints can cause problems with the accuracy of structural predictions. Both the DMC and MRMP calculations were performed at geometries that were obtained with other methods, since analytic gradients are not currently available for either method.
2. The DMC calculations made use of the fixed-node approximation, in which the nodal surfaces are fixed at those of a trial wave function.

CASSCF calculations on the $Si_{15}H_{16}$ cluster model, using the geometries of Filippi et al., predict the planar structure to be more stable (just as is found for our CASSCF-optimized structures). For the $Si_{15}H_{16}$, and $Si_{21}H_{20}$ cluster models, for which the DMC calculations favor the buckled structures, Hartree-Fock trial functions were employed in the DMC calculations. This could introduce a bias toward the buckled structures, as the use of Hartree-Fock trial wave functions should be more appropriate for the buckled structures.

Aside from errors due to the fixed-node approximation, the DMC method should recover all the correlation energy in the system, if the calculations are run sufficiently long, and at appropriate geometries. Likewise, the accuracy of the MRMP2 method relies on the convergence of the perturbation expansion, so this method may not include high-order correlation effects. In general the MRMP2 method has proven to be quite successful for treating systems with considerable diradical character. However, given the small energy differences involved we cannot rule out the possibility that (a) correlation effects missing in the MRMP2 method, (b) the HF trial functions and fixed-node approximations used in the DMC study, and (c) the lack of analytic gradients for both methods could play some role in determining the relative stability of planar and buckled structures of the cluster models considered here.

Conclusion

The structure of the Si(100) surface was investigated using two-dimer ($Si_{15}H_{16}$), three-dimer ($Si_{20}H_{21}$) and five-dimer ($Si_{33}H_{28}$) surface cluster models. Because of the radical-like dangling bonds of the surface dimers, multi-reference wave functions were used to recover the quasi-degenerate non-dynamic electron correlation. CASSCF(4,4), CASSCF(6,6) and CASSCF(10,10) geometry optimizations for the two- three- and five-dimer clusters all generate only a symmetric structure as a minimum. This implies that dimer-dimer interactions do not play a major role in determining the structure of the surface. An analysis using CASSCF localized orbitals suggests that even though inter-dimer repulsions do decrease upon buckling, this effect is more than compensated by the preference of partial π bonding for the symmetric structure. The comparison of the dimer bond lengths for different cluster models shows that the dimer bond length is independent of cluster models as long as a proper multi-reference wave function is used. In order to further recover the dynamic part of the correlation, MRMP2 single point calculations were performed along the buckling normal modes. The MRMP2 results are consistent with the prediction of symmetric (or unbuckled) structures, although the distortion energies associated with surface buckling decreases somewhat when going from CASSCF to MRMP calculations.

It is important to emphasize that although these calculations address clusters of increasing size, they are still clusters of finite size, a size that would be considered to be small when compared with the bulk. So, while the calculations presented here suggest that finite clusters, when investigated using adequate wave functions, appear to be symmetric (unbuckled), it is not clear to what degree that these results can be extrapolated to the bulk. In this regard, it is worth noting that a recently developed hybrid quantum mechanics/molecular mechanics method [12], the surface integrated molecular orbital molecular mechanics (SIMOMM) method provides a computationally inexpensive approach to studying very large clusters. This method has recently been used to study cyclohexadiene [20], water [21], and atomic oxygen [35] on the Si(100) surface. We are currently exploring using the SIMOMM method to explore larger Si(100) cluster models than can be realistically studied with quantum chemistry alone. Finally, one would also like to explore entropy contributions to the relative energetics of the surface as it buckles. This is a challenging problem, since the low frequency buckling modes, which will make large contributions to the entropy, are not likely to be adequately treated with the harmonic approximation that is present in most electronic structure packages. So, more sophisticated alternatives will be required [36, 37, 38, 39, 40, 41, 42, 43].

Acknowledgements. This work was supported in part by a grant from the Air Force Office of Scientific Research. The calculations reported here were performed on an Alpha Cluster, obtained by grants from the Department of Energy and the National Science Foundation, and on the IBM SP2 at the Maui High Performance Computation Center through a DoD Grand Challenge grant. The authors thank Dr. Michael Schmidt for many helpful discussions. We thank Dr. Filippi for sending us the geometries used in her DMC calculations.

References

1. Wu CJ, Carter EA (1992) Phys Rev B 45: 9065
2. Goddard WA III, McGill TC (1979) J Vac Sci Technol 16:1308
3. Rappe AK, Smedley TA, Goddard WA III (1981) J Phys Chem 85:1662
4. Kratzer P, Hammer B, Korskov JK (1993) Phys Rev B 51:13432
5. Vittandi A, Selloni A, Casarin M (1993) Surf Sci 289:265
6. Neergaard H, Yates JT (1995) Chem Rev 95:1589
7. Tromp RM, Hamers RJ, Demuth HE (1985) Phys Rev Lett 55:1303 ; Hamers RJ, Avouris Ph, Bozso F (1987) ibid 59:2071; Hamers RJ, Avouris Rh, Bozso F (1988) J Vac Sci Technol A 6:508
8. Schmidt MW, Gordon MS (1998) Annu Rev Phys Chem 4:233
9. Redondo A, Goddard WA III (1982) J Vac Sci Technol 21:344
10. Paulus B (1997) Surf Sci 375:55
11. Shoemaker J, Burggraf JW, Gordon MS, (2000) J Chem Phys 112:2994
12. Gordon MS, Shoemaker JR, Burggraf LW (2000) J Chem Phys 113:9355
13. Hess JS, Doren DJ (2000) J Chem Phys 113:9353
14. Konecny R ,Doren DJ (1997) J Chem Phys 106: 2426
15. Yang C,Kang HC (1999) J Chem Phys 110:11029
16. Penev E, Kratzer P, Scheffler M (1999) J Chem Phys 110:3986
17. Yang C, Lee SY, Kang HC (1997) J Chem Phys 107:3295
18. Steckel JA, Phung T, Jordan KD, Nachtigall P (2001) J Phys Chem B 105:4031
19. Hehre WJ, Ditchfield R, Pople JA (1972) J Chem Phys 56:2257; Francl MM, Pietro WJ, Hehre WJ, Binkley JS, Gordon MS, Defrees DJ, Pople JA (1982) ibid 77:3654
20. Choi CH, Gordon MS (1999) J Am Chem Soc 121:11311
21. Jung Y, Choi CH, Gordon MS (2001) J Phys Chem B 105:4039
22. Hay PJ, Wadt WR (1985) J Chem Phys 82:270; Hay PJ, Wadt WR (1985) J Chem Phys 82:284; Hay PJ, Wadt WR (1985) J Chem Phys 82:299
23. Nakano H (1993) J Chem Phys 99:7983
24. Schmidt MW, Baldridge KK,Boatz JA, Elbert ST, Gordon MS, Jensen JH, Koseki S, Matsunaga N, Nguyen KA, Su S, Windus TL, Dupuis M, Montgomery JA Jr (1993) J Comput Chem 14:1347
25. Windus TL, Schmidt MW,Gordon MS (1994) Theor Chim Acta 89:77
26. Alexeev Y, Gordon MS (2003) (in preparation)
27. Wang Y, Shi M, Rabalais JW (1993) Phys Rev B, 48: 1689
28. Edmiston C, Ruedenberg K (1963) Rev Mod Phys 35:457
29. Raffenetti RC, Ruedenberg K, Janssen CL, Schaefer HF (1993) Theor Chim Acta 86:149
30. Wolkow RA (1992) Phys Rev Lett 68:2636
31. Pehlke E, Scheffler M (1993) Phys Rev Lett 71:2338
32. Yokoyma T, Takayanagi K (2000) Phys Rev B 61:R5078,
33. Badt D, Wengelnik H, Neddermeyer H (1994) J Vac Sci Technol B 12:2015
34. Healy SB, Filippi C, Kratzer P, Penev E, Sheffler M (2001) Phys Rev Lett 87:16105
35. Choi CH, Liu D-J, Evans J, Gordon MS(2003) J Am Chem Soc (submitted)
36. Chaban GM, Jung JO, Gerber RB (1999) J Chem Phys 111:1823
37. Bowman JM (1978) J Chem Phys 68:608
38. Gerber RB, Ratner MA (1979) Chem Phys Lett 68:195
39. Bowman JM (1986) Acc Chem Res 19:202
40. Gerber RB Ratner MA (1998) Adv Chem Phys 70:97
41. Jung JO, Gerber RB (1996) J Chem Phys 105:10332
42. Norris LS, Ratner MA, Roitberg AE, Gerber RB (1996) J Chem Phys 106:11261
43. Yagi K, Taketsugu T, Hirao K, Gordon MS (2000) J Chem Phys 113:105
44. Wang Y, Shi M, Rabalais JW (1993) Phys Rev B 48, 1689